Biochimica et Biophysica Acta 1808 (2011) 171–182

Contents lists available at ScienceDirect

Biochimica et Biophysica Acta

journal homepage: www.elsevier.com/locate/bbamem

A plausible mode of action of pseudin-2, an antimicrobial peptide from *Pseudis paradoxa*

Seong-Cheol Park [a], Jin-Young Kim [a], Chanyoung Jeong [a], Suyeon Yoo [c], Kyung-Soo Hahm [a,b,*], Yoonkyung Park [a,c,*]

[a] Research Center for Proteinaceous Materials (RCPM), Chosun University, Gwangju, Republic of Korea
[b] Department of Cellular·Molecular Medicine School of Medicine, Chosun University, Gwangju, Republic of Korea
[c] Department of Biotechnology and BK21 Research Team for Protein Activity Control, Chosun University, Gwangju, Republic of Korea

ARTICLE INFO

Article history:
Received 30 April 2010
Received in revised form 23 August 2010
Accepted 30 August 2010
Available online 6 September 2010

Keywords:
Antimicrobial peptide
pseudin-2
Giant unilamellar vesicle
Toroidal pore
Depolarization
Penetration
RNA-binding

ABSTRACT

The search for new antibiotic agents is continuous, reflecting the continuous emergence of antibiotic-resistant pathogens. Among the new agents are the antimicrobial peptides (AMPs), which have the potential to become a leading alternative to conventional antibiotics. Studies for the mechanisms of action of the naturally occurring parent peptides can provide the structural and functional information needed for the development of effective new antibiotic agents. We therefore characterized pseudin-2, an AMP isolated from the skin of the South American paradoxical frog *Pseudis paradoxa*. We found that pseudin-2 organized to an aggregated state in aqueous solution, but that it dissociated into monomers upon binding to lipopolysaccharide (LPS), even though it did not neutralize LPS in Gram-negative bacteria. In addition, pseudin-2 assumed an α-helical structure in the presence of biological membranes and formed pores in both bacterial and fungal membranes, through which it entered the cytoplasm and tightly bound to RNA. Thus, the potent antimicrobial activity of pseudin-2 likely results from both the formation of pores capable of collapsing the membrane potential and releasing intracellular materials and its inhibition of macromolecule synthesis through its binding to RNA.

1. Introduction

As the problem of bacterial resistance has increased over the years, small proteins and peptides with antimicrobial properties have attracted attention as the basis for antibiotic drug design. Among these, AMPs are evolutionarily ancient antimicrobial weapons widely distributed throughout the animal and plant kingdoms [1]. To date, several thousand AMPs have identified in nature, designed *de novo* and produced synthetically. Common features of these peptides include a positive net charge under physiological conditions, amphipathic secondary structures within membranes, small size and rapid binding to biological membranes, usually killing within minutes [1,2]. Although their mode of action is not well understood, it is believed that multiple targets are the disruption of cytoplasmic membrane and the processes of cell division and macromolecule synthesis [2]. Most of antimicrobial peptides are known to cause the efflux of intracellular materials by destabilizing or disrupting the cytoplasmic membrane via either mechanism of pore formation through "barrel-stave" and "toroidal pore" or nonpore "carpet-like" mechanism [3–6]. Furthermore, to reach their intracellular targets, which are nucleotides and functional proteins, they must permeate the cell wall and cytoplasmic membrane.

Granular glands in the skins of frogs and toads are rich in bioactive peptides that protect the animals against pathogenic microorganisms [5,7]. Since the first known amphibian AMP was identified in the skin of the European frog *Bombina variegate* about 30 years ago, over 500 peptides have been found in frogs and toads [7]. Pseudin-2 (GLNALKKVFQGIHEAIKLINNHVQ-NH_2) is an AMP isolated from the skin of the South American paradoxical frog *Pseudis paradoxa* [8]. In previous studies, pseudin-2 was shown to exert a potent growth inhibitory effect against Gram-negative bacteria [8] and to stimulate insulin secretion via a Ca^{2+}-independent mechanism, suggesting it could potentially serve as the basis for the development of insulinotropic agents for the treatment of type-2 diabetes [9]. With that as background, the aim of the present study was to determine the mode of antimicrobial action of pseudin-2, and then to gain a basic understanding of the relation between the structure of pseudin-2 and its antimicrobial action.

* Corresponding authors. Research Center for Proteinaceous Materials (RCPM), Chosun University, Gwangju, Republic of Korea. Tel.: +82 62 230 7556; fax: +82 62 227 8345.
E-mail addresses: kshahm@chosun.ac.kr (K.-S. Hahm), y_k_park@chosun.ac.kr (Y. Park).

0005-2736/$ – see front matter © 2010 Elsevier B.V. All rights reserved.
doi:10.1016/j.bbamem.2010.08.023

2. Materials and methods

2.1. Materials

Fluorescein isothiocyanate-labeled dextrans with average molecular masses of 4, 10, 20, and 40 kDa (FD-4/ 10/ 20/ 40), ergosterol and proteinase K were purchased all from Sigma Chemical Co. (St. Louis, MO). L-α-phosphatidylethanolamine (PE), sphingomyelin (SM), cholesterol (CH), L-α-phosphatidyl-DL-glycerol (PG) and L-α-phosphatidylcholine (PC) were from Avanti Polar Lipids (Alabaster, AL). 3,3'-diethylthio-dicarbocyanine iodide ($DiSC_3$-5), 4-fluoro-7-nitrobenz-2-oxa-1,3-diazole (NBD-F), carboxy-tetramethylrhodamine succinimidyl ester (rhodamine-SE) and calcein were from Molecular Probes (Eugene, OR). 9-fluorenyl-methoxycarbonyl (Fmoc) amino acids were from CEM Co. All other reagents were of analytical grade.

2.2. Microorganisms

Escherichia coli (ATCC 25922), *Staphylococcus aureus* (ATCC 25923), *S. epidermidis* (ATCC 12228) and *Pseudomonas aeruginosa* (ATCC 15692) were obtained from the American Type Culture Collection. *Bacillus subtilis* (KCTC 1998), *B. megaterium* (KCTC 3709), *Listeria monocytogenes* (KCTC 3710), *Enterobacter cloacae* (KCTC 2361), *Klebsiella pneumoniae* (KCTC 2208), *Salmonella typhimurium* (KCTC 1926), *Aspergillus parasiticus* (KCTC 6598), *A. flavus* (KCTC 6905), *Penicillium verrucosum* (KCTC 6265), *Candida albicans* (KCTC 7270) and *Trichosporon beigellii* (KCTC 7707) were from the Korean Collection for Type Cultures. *E. coli* CCARM 1229, *E. coli* CCARM 1238, *S. aureus* CCARM 3089, *S. aureus* CCARM 3114, *S. typhimurium* CCARM 8009 and *S. typhimurium* CCARM 8013 were distributed from Culture Collection of Antibiotics Resistance Microbes at the Seoul Women's University, Korea. *P. aeruginosa* 4007, 3547 and 4891 were resistant strains isolated from patients with otitis media in a hospital.

2.3. Peptide synthesis

Peptides were synthesized using Fmoc solid-phase methods on Rink amide 4-methyl benzhydrylamine resin (Novabiochem) (0.55 mmol/g) with a Liberty microwave peptide synthesizer (CEM Co. Matthews, NC). The fluorescent labeling of the N-terminals of peptide was performed with NBD-F in DMF or rhodamine-SE in DMF (3–4 eq.) containing 5% (v/v) diisopropylethylamine [10,11]. After purification of synthetic peptides through reversed-phase HPLC on C_{18} column, the molecular masses of the peptides were confirmed using a matrix-assisted laser desorption ionization mass spectrometer (MALDI II, Kratos Analytical Ins.) [12].

2.4. Antibacterial activity

Bacterial cells were cultured at 37 °C in appropriate culture media. The antimicrobial activities of peptides were determined in microdilution assays. Briefly, microorganisms were collected during their mid-log phase and suspended in buffer I (low ionic strength buffer; 10 mM sodium phosphate, pH 7.2) or buffer II [high ionic strength buffer; PBS (1.5 mM KH_2PO_4, 2.7 mM KCl, 8.1 mM Na_2HPO_4, 135 mM NaCl, pH 7.2)] supplemented with 10 % culture media. Aliquots of the cell suspension (5×10^5 colony forming unit/ml) were added to each well with two-fold serial dilutions of each peptide and the samples were then incubated at 37 °C for 24 h. Minimum inhibitory concentrations (MICs) of peptides were obtained by measuring the turbidity of each well at the absorbance at 600 nm. The lowest concentration of peptide that completely inhibited bacterial growth was defined as the MIC [12].

2.5. Antifungal activity

To assess the activity of pseudin-2 against various fungal pathogens, fungal spores from 10-day-old cultures grown on PDA plates at 28 °C were collected using 0.08% Triton X-100. Yeast cultures grown overnight were then suspended in medium comprised of half YPD medium and half appropriate buffer. A spore (conidia) suspension (final concentration 10^4 spores/ml) in PD media were mixed with 20 μl of peptides. After incubating for 24 to 36 h at 28 °C, the lowest concentration of peptide inhibiting the growth and germination of fungi was microscopically determined as the MIC [13].

2.6. Hemolysis and cytotoxicity

The hemolytic activity against fresh human red blood cells (hRBCs) and cytotoxic activity against HaCaT (human keratinocyte) and NIH/3T3 (mouse fibroblast) cells were examined according the method previously described [12,13].

2.7. Circular dichroism (CD)

CD spectra were recorded at 25 °C on a Jasco 810 spectropolarimeter (Jasco, MD, USA) equipped with a temperature control unit. A quartz cell with 0.1 cm path-length was used with a 30-μM peptide solution under the indicated conditions [various concentrations of peptide and NaCl, 50% trifluoroethanol (TFE, v/v), 120 μM LPS, and 1.5 mM liposomes (PE/PG, 7:3, mol/mol and PC/PE/PI/ergosterol, 5:4:1:2, mol/mol)]. Five scans from to 190–250 nm were acquired for each condition and averaged to improve the signal to noise ratio. Mean residue ellipticities ($[\theta]$, deg·cm^{2}dmol^{-1}) were calculated using Eq. (1) [14,15]:

$$[\theta] = \theta_{obs} / 10 \cdot l \cdot c \quad (1)$$

where θ_{obs} is the measured signal (ellipticity) in millidegrees, l is the optical path-length of the cell in cm, and c is the concentration of peptide in mol/L [mean residue molar concentration: c = number of residues in the constructed of peptide × the molar concentration of the peptide].

2.8. Aggregated states of peptides in solution

Fluorescence emission from tetramethylrhodamine (TAMRA)-labeled peptides (0.05–1 μM) was monitored in 1 ml of PBS. The fluorescence emission (575 nm) was increased by dequenching the rhodamine fluorescence excited at 530 nm by incubation for 2 h in proteinase K (10 μg/ml). All subsequent fluorescence measurements were made at room temperature on a Perkin-Elmer LS-55 spectrofluorimeter [16].

2.9. Membrane depolarization

Membrane depolarization was assessed using Dis-C_3-5, a lipophilic potentiometric indicator dye, with intact *E. coli* cells as previously described [12,17].

2.10. SYTOX green uptake

E. coli cells were grown to mid-logarithmic phase at 37 °C, washed, and suspended in PBS buffer (2×10^7 cells/ml) containing 10% LB medium, after which they were incubated with 1 μM SYTOX green for 15 min in the dark [18]. After addition of the peptides to the indicated concentrations, the time-dependent increase of fluorescence excited by the binding of the cationic dye to intracellular DNA was monitored. The excitation and emission wavelengths were 485 nm and 520 nm, respectively.

2.11. Time-kill kinetics of peptides

Suspensions of *E. coli* (OD_{600} 0.05) were added to peptide solutions containing the same concentrations of peptide used in the membrane depolarization experiment. The bacteria were then exposed to the peptides at 2× or 4× the MIC for 0, 2, 4, 6, 8, 10, 15, 20, 30, 40 or 60 min, after which they were diluted 20-fold, plated on Luria broth agar (LA), and incubated overnight before counting the colonies [19].

2.12. Effects of lipopolysaccharide on antibacterial activity

Peptides diluted serially to concentrations ranging from 8 to 256 μM were mixed with 256 μM LPS (*E. coli* 055:B5, Sigma) (peptide: polysaccharides ratio = 1:1–32). After incubation for 1 h at 37 °C, suspensions of exponentially growing *S. aureus* were added to the mixtures. The plates were then incubated for 4 h at 37 °C, after which aliquots were dripped onto MH agar plates and incubated for an additional 24 h [20].

2.13. Aggregation states of peptides in LPS

To evaluate the association or dissociation of TAMRA-peptides in LPS, the time-dependent dequenching of rhodamine fluorescence was measured [21]. Briefly, TAMRA-peptides were added to 1 ml of PBS to a final concentration of 1 μM, after which LPS was added to the indicated peptide/LPS molar ratio. After 15 min, proteinase K (80 μg/ml) was added, and the change in fluorescence emission intensity was monitored. The excitation and emission wavelengths were 485 and 590 nm, respectively.

2.14. Confocal laser-scanning microscopy (CLSM)

To determine the cellular distribution of pseudin-2, *E. coli* and *C. albicans* incubated with TAMRA-pseudin-2 of 1× or 2× the MIC were observed on a CLSM. After incubation for 30 min, the cells were washed three times with ice-cold PBS buffer and then pre-incubated with Hoechst 33258 (Molecular Probes, OR, USA) to label cytoplasmic DNA in cell suspensions of *C. albicans*. Localization of TAMRA-pseudin-2 was then examined using an inverted LSM510 laser-scanning microscope (Carl Zeiss, Göttingen, Germany). To simultaneously detect intracellular TAMRA-pseudin-2 and Hoechst 33258, the 405-nm light from a diode laser and 543-nm light from a helium neon laser were directed at a UV/488/543/633 beam splitter. Images were then recorded digitally in a 512 × 512 pixel format [22].

2.15. Accessibility of membrane-bound peptides

Lipid vesicles (50 μM) were added to NBD-labeled peptides (0.1 μM). After 15 min, proteinase K (10 μg/ml) was added, and fluorescence intensity was recorded before and after the addition of enzyme. The excitation and emission wavelengths were 470 nm and 530 nm, respectively [23].

2.16. Calcein leakage

The permeabilizing activity of peptides was assayed by measuring calcein leakage from large unilamellar vesicles (LUVs) with entrapped calcein according to method described previously [12,24].

2.17. Preparation and visualization of giant unilamellar vesicles (GUVs)

GUVs were prepared using the electroformation method originally developed by Angelova and Dimitrov [25,26]. Briefly, phospholipid mixtures were prepared in chloroform-methanol (9/1). The following mixtures were used: PE/PG/rhodamine-PE (69/30/1) and PC/PE/PI/ergosterol/rhodamine-PE (50/39/10/20/1) for fluorescently-labeled liposomes; and PE/PG (7/3) and PC/PE/PI/ergosterol (5/4/2/1) for carboxyfluorescein (CF)-containing liposomes. Two hundred fifty microliters of lipid mixture were deposited onto indium tin oxide (ITO)-coated glass slides (25 × 35 × 1.1 mm, Sigma-Aldrich, St. Louis, MO), which were then spin-coated at 600 rpm for 6 min. The residual organic solvents were removed by evacuation in a vacuum for at least 2 h. Two ITO glass slides (one with a lipid film) were separated by a poly(dimethylsiloxane) spacer in order to form an electroformation chamber (25 × 25 × 1 mm). The chamber was then filled with 5 mM HEPES buffer containing 0.1 M sucrose with or without 6 μM CF (for fluorescently-labeled liposomes and CF-containing liposomes, respectively) through a hole in the poly(dimethylsiloxane) spacer. A 1.7 V (peak to peak), 10 Hz AC field was then immediately applied to the ITO slides using a function generator (Agilent 33220A, Agilent Technology, US). After 1.5 h, the electric field was changed to 4 V, 4 Hz for 10 min to detach the liposomes that formed on the slides. The liposome solution was gently removed from the electroformation chamber, and aliquots were diluted in 5 mM HEPES buffer containing 0.1 M glucose. Aliquots of the resultant GUV suspension were then deposited on microscope slides and allowed to settle for 1 min. This settling was due to the density difference between the sugar solutions inside and outside the liposomes. The liposomes were then examined under an inverted fluorescence phase contrast microscope (IX71, Olympus, Tokyo, Japan), and images were recorded using a digital CCD camera (DP71, Olympus) and video recorder, and analyzed using software provided by the manufacturer.

2.18. Estimation of pore size in live cells and artificial liposomes

Soluble fluorescent molecules, including calcein (Mw, 623; diameter, ~1 nm), FD4 (Mw, 3.9 kDa; diameter, ~2.8 nm), FD10 (Mw, 9.9 kDa; diameter, ~4.6 nm), FD20 (Mw, 19.8 kDa; diameter,

Table 1
Antimicrobial activity of pseudin-2.

Microorganism	MIC (μM)				
	Pseudin-2	Melittin	Amp	Ery	Cip
G(+) Bacteria					
L. monocytogenes	4 (8)	4 (8)	–	–	–
S. aureus	32 (128)	2 (2)	–	4	–
B. subtilis	2 (4)	1 (2)	–	–	–
B. megaterium	2 (4)	2 (4)	–	–	–
S. epidermidis	32 (64)	2 (8)	–	–	–
G(−) Bacteria					
E. coli	2 (4)	2 (4)	64	–	0.25
P. aeruginosa	8 (16)	4 (8)	–	–	0.25
S. typhimurium	2 (4)	4 (8)	32	–	–
E. cloacae	2 (4)	2 (4)	–	–	–
K. pneumoniae	2 (4)	2 (4)	–	–	–
Yeast					
C. albicans	8 (16)	8 (16)	–	–	–
T. beigellii	8 (16)	4 (16)	–	–	–
Fungi					
A. farasiticus	16 (32)	16 (32)	–	–	–
A. flavus	32 (64)	32 (64)	–	–	–
P. verrucosum	8 (16)	4 (16)	–	–	–
Resistant strains					
S. aureus CCARM 3089	16 (128)	2 (2)	-	>512	–
S. aureus CCARM 3114	16 (128)	2 (2)	-	>512	-
S. typhimurium CCARM 8009	4 (8)	2 (4)	>512	–	–
S. typhimurium CCARM 8013	2 (8)	1 (4)	>512	–	–
E. coli CCARM 1229	1 (4)	1 (2)	>512	–	512
E. coli CCARM 1238	1 (4)	2 (4)	>512	–	512
P. aeruginosa 4007	4 (8)	1 (2)	–	–	256
P. aeruginosa 3547	4 (8)	2 (4)	–	–	256
P. aeruginosa 4891	4 (8)	2 (4)	–	–	256

*Antimicrobial assays were performed in 10 mM sodium phosphate (low ionic strength buffer) and PBS (high ionic strength buffer, number in the parenthesis). *P. aeruginosa* 4007, 3547 and 4891 are resistant-strains isolated from patients with otitis media in a hospital. Amp, Ery, and Cip are ampicillin, erythromycin and ciprofloxacin, respectively.

~6.6 nm) and FD40 (Mw, 40.5 kDa; diameter, ~9 nm), were added to *E. coli* or *C. albicans* cells to final concentrations of 2 μM, 0.1 mg/ml, 0.1 mg/ml, 0.2 mg/ml and 0.1 mg/ml, respectively. A peptide mixture containing 2% rhodamine-labeled peptide was then added to a final concentration of 4 μM (*E. coli*) or 16 μM (*C. albicans*). After incubation for 10 min, the influx of fluorescent molecules was examined using CLSM. A 2% rhodamine-labeled peptide was also used to visualize the binding of peptide to the cell surface [27].

In addition, to estimate the size of pores in artificial vesicles, soluble fluorescent molecules (calcein, FD-4, -10, -20 and -40) served as models of cytoplasmic components. Unilamellar vesicles having different lipid compositions and entrapping FD were prepared using the reverse-phase evaporation method [12,28], and the experiment was performed as described previously [12]. In all experiments, the concentration of vesicles was determined in triplicate using a phosphorus assay [29].

2.19. DNA/RNA gel retardation

Plasmid pBluescript SK(+) (Stratagene) and pTYB2 (NEB Inc.) were purified using a plasmid extraction kit (Exprep™ Quick, GeneAll Biotechnology Co., Seoul, Korea), and yeast RNA was isolated using TRI reagent (MRC inc. Cincinnati, OH). The plasmid DNA (200 ng) or yeast RNA (10 μg) was mixed with increasing amounts of peptides in 10 mM Tris buffer (pH 8.0) containing 1 mM EDTA, 5% glycerol, 20 mM KCl and 50 μg/ml BSA. The mixtures were incubated for 10 min at 37 °C and then electrophoresed on a 0.5% or 1% agarose gel in the TBE buffer, after which the gels were stained with ethidium bromide [30]. Gel retardation was visualized under UV illumination using a Bio-Rad Gel Documentation system.

3. Results

3.1. Lytic effects of pseudin-2

In this study, we used *in vitro* assays to measure the antimicrobial activity of pseudin-2 against five strains of Gram-negative bacteria, Gram-positive bacteria and fungal cells, and against nine strains of antibiotic-resistant bacteria. As a positive control, we also tested the effects of melittin, a known AMP. As shown in Table 1, the MICs of pseudin-2 ranged from 2 to 4 μM (in low ionic strength buffer) against nearly all bacterial strains, except *P. aeruginosa*, against which it had a MIC of 8 μM. Antimicrobial activities of two peptides were slightly inhibited in the presence of high ionic strength buffer. In addition, the MICs for *S. aureus* were 32 and 128 μM (low and high ionic strength buffer, respectively), which were higher than for other bacteria. Pseudin-2 also exerted potent antimicrobial activity against antibiotic-resistant bacteria and pathogenic fungal cells.

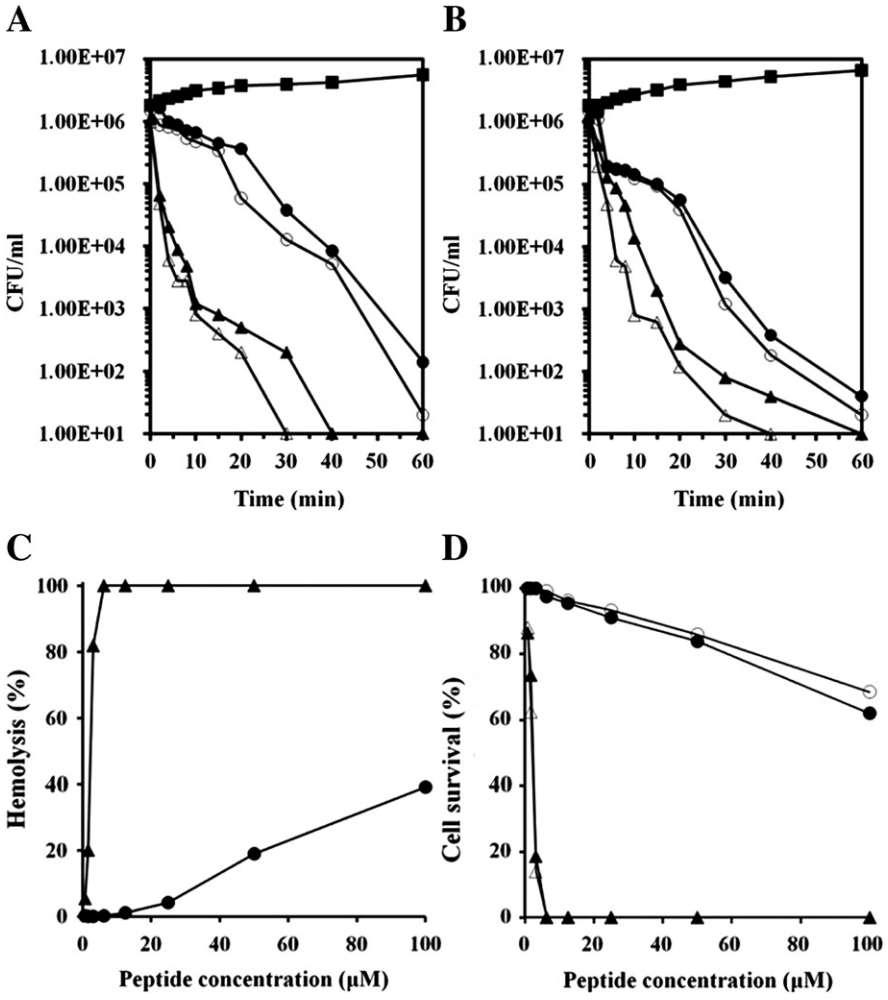

Fig. 1. Time-kill kinetics of AMPs against *E. coli* strains and cytotoxicity toward hRBC, NIH/3 T3 cells and HaCaT cells. (A and B) *E. coli* (A) and *E. coli* CCARM 1238 (B) were incubated with pseudin-2 (●) or melittin (▲) at 2× (white) and 4× (black) their MIC values for the indicated times. Squares show the normal growth in the absence of an AMP. (C) Dose-dependent release of hemoglobin measured after incubating hRBCs (8% hematocrit) for 1 h with pseudin-2 (●) or melittin (▲). (D) NIH/3 T3 (filled) or HaCaT (open) cells (4×10^3 cell/well) were incubated for 24 h with the indicated concentrations of pseudin-2 (circles) or melittin (triangles), after which percent cell survival was determined in MTT assays. All graphs show means ± SEM of values obtained from at least two independent experiments performed in duplicate.

To determine whether the antibacterial action of pseudin-2 is bacteriocidal or growth-inhibiting, we next assessed its time-kill kinetics. Fig. 1A and B show time-kill curves for pseudin-2 and melittin, respectively, at 2× and 4× the MICs for *E. coli* ATCC 25922 (antibiotic-sensitive strain) and *E. coli* CCARM 1238 (antibiotic-resistant strain). Although the two peptides exhibited similar bactericidal actions against the two *E. coli* strains, pseudin-2 reduced the viable bacterial population more slowly than melittin: whereas melittin elicited a significant reduction in viable bacteria within 15 min, pseudin-2 did so within 30 min.

The cytotoxicities of pseudin-2 and melittin were tested against hRBCs, NIH/3T3 cells and HaCaT cells (Fig. 1C and D). Incubating hRBCs for 1 h in the presence of 100 μM pseudin-2 resulted in 39% cell lysis. The same concentration of pseudin-2 caused 38% and 30% cytotoxicity in NIH/3T3 and HaCaT cells, respectively. Melittin showed 100% lysis at 6.25 μM (Fig. 1C).

3.2. Helical self-association of pseudin-2 in aqueous solution

To characterize the structure and organization of pseudin-2 in aqueous solution, we initially determined the secondary structure in buffer from CD spectra. The far-UV CD spectra in Fig. 2A and B show the effects of increasing the concentration of pseudin-2 or NaCl in 10 mM sodium phosphate buffer. Increasing the peptide concentration induced an α-helical structure of pseudin-2, suggesting the peptide self-associates in aqueous solution. Increasing the ionic strength, by contrast, had no effect on the secondary structure of pseudin-2.

To further investigate the properties of the apparently self-associated pseudin-2, we labeled pseudin-2 and melittin at their N-termini with rhodamine (Rho-pseudin-2 and Rho-melittin, respectively), which is somewhat sensitive to the polarity of its environment but does not disturb the peptides' biological function. This was based on the self-quenching of rhodamine fluorescence, which occurs when rhodamine-labeled peptides are in close proximity, to assess the degree to which rhodamine-labeled peptides aggregate in solution. That is, if there is substantial aggregation of rhodamine-labeled peptides aggregate, cleavage by a proteolytic enzyme, leading to their dissociation, will cause a pronounced increase in rhodamine fluorescence. Rho-pseudin-2 (0.2 μM) initially emitted less fluorescence than Rho-melittin in sodium phosphate buffer. However, after the addition of proteinase K, which degraded the peptides, much larger increases in fluorescence were seen with Rho-pseudin-2 than Rho-melittin (Fig. 2C). These suggest that pseudin-2 adopts α-helical structure and is highly self-associated in aqueous solution.

3.3. Concentration-dependent localization of pseudin-2

To determine the target site of pseudin-2 prior to functional studies, Rho-pseudin-2 was incubated with *E. coli* or *C. albicans* at 1× and 2× the MIC, after which its distribution was visualized by CLSM. We observed two distinct cell populations with Rho-pseudin-2 respectively localized at the cell surface or in the cytoplasm, depending on the peptide concentration (Fig. 3). It appeared that Rho-pseudin-2 at the MIC accumulated more on the surfaces of cells than in the cytoplasm, while the reverse was true at 2× the MIC. In *C. albicans*, moreover, double labeling with Rho-pseudin-2 and the DNA probe Hoechst 33258 revealed that cytoplasmic Rho-pseudin-2 localized around nucleic acids, suggesting it interacts with DNA or RNA (Fig. 3C).

3.4. Effects of LPS on the organization and antimicrobial activity of pseudin-2

To better understand the interaction and organization of pseudin-2 as it penetrates the cell wall, we measured Rho-pseudin-2 fluorescence before and after the addition of LPS. Rho-pseudin-2 fluorescence increased after addition of LPS, even at low concentrations of LPS

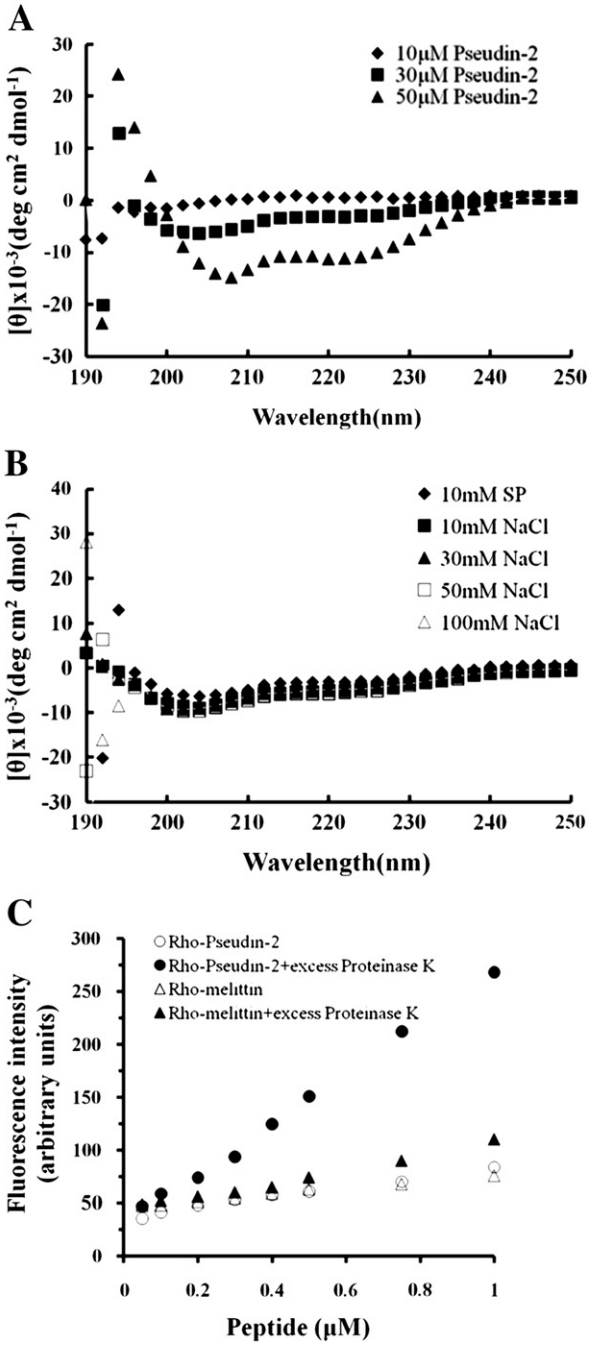

Fig. 2. CD spectra and self-association of peptides in aqueous solution. (A and B) Far-UV CD spectra obtained at the indicated pseudin-2 concentrations in PBS (A) and at 30 μM pseudin-2 in 10 mM sodium phosphate buffer with the indicated NaCl concentrations (B) are expressed as mean molar residue ellipticity (θ). (C) Self-association (or aggregation) of Rho-pseudin-2 and Rho-melittin detected indirectly based on increases of fluorescence intensity in PBS induced by incubation for 2 h with or without proteinase K. The excitation and emission wavelengths were 530 and 582 nm, respectively.

(peptide/LPS molar ratio of 1:1; Fig. 4A), although this was slightly decreased at molar ratio of 1:32. After addition of proteinase K (arrow 2 in Fig. 4A), the fluorescence increased significantly, as it did in the absence of LPS. This suggests that self-aggregated pseudin-2 peptides are dissociated by LPS, after which free pseudin-2 formed random complexes with LPS, which did not neutralize the LPS (supplementary Fig. 1). We also confirmed the effect of LPS on the antibacterial activity of peptides using *S. aureus* (Fig. 4B). Pseudin-2 pre-incubated with LPS retained nearly all of its lytic activity against *S. aureus*, indicating that pseudin-2 bound to LPS continues to act as a free peptide.

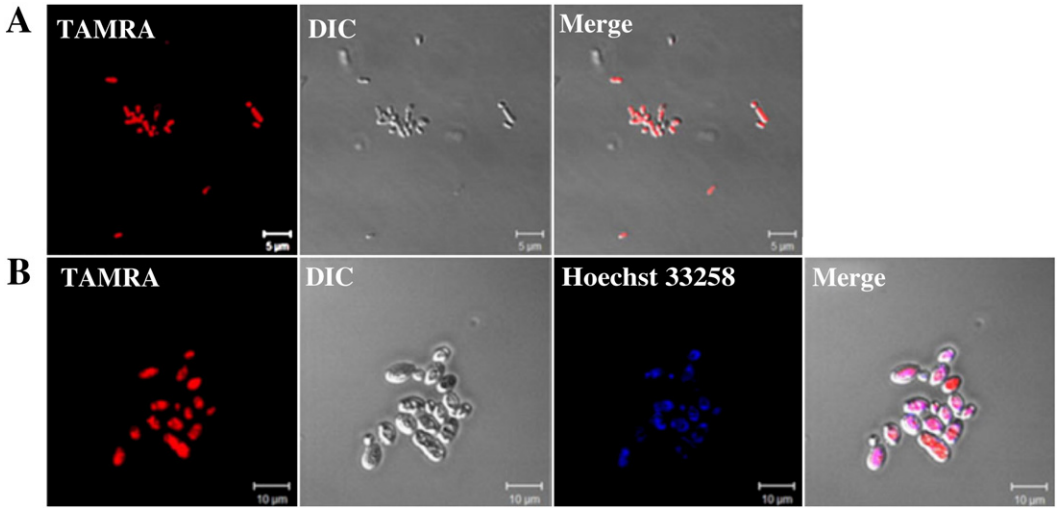

Fig. 3. Concentration-dependent localization of pseudin-2. *E. coli* (A) and *C. albicans* cells (B) were incubated for 10 min with Rho-pseudin-2 at its MIC and then observed under CLSM. To confirm intracellular localization of the peptide, *C. albicans* cells were preincubated with Hoechst 33258 before addition of Rho-pseudin-2.

3.5. Pseudin-2-induced membrane disruption

We next assessed pseudin-2-induced membrane alterations and disruption in *E. coli* cells using two complementary assays: (1) detection of membrane depolarization using $DisC_35$, a lipophilic potentiometric indicator dye (Fig. 5A and B), and (2) entrance of the vital dye SYTOX Green into cells, indicating permeation of the cytoplasmic membrane (Fig. 5C and D).

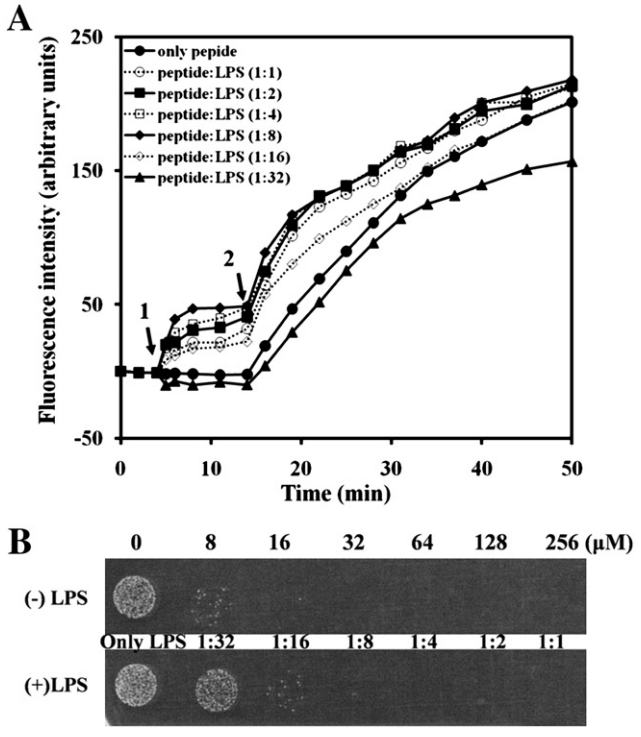

Fig. 4. The effects of LPS and LTA on the organization (A) and antibacterial activity (B) of pseudin-2. (A) *E. coli* O111:B4 LPS (arrow 1) were added to the indicated molar ratio when fluorescence of the labeled peptide reached a steady state. The excitation and emission wavelengths were 485 nm and 590 nm, respectively. After 10 min, proteinase K was added (arrow 2). (B) Peptides were pre-incubated with LPS at the indicated molar ratios. The exponential phase bacteria (*S. aureus*) were then added to the mixtures. After incubation for 4 h, aliquots were withdrawn and plated on agar plates.

Membrane depolarization measured in intact bacterial cells was monitoring the increase of $DisC_35$ fluorescence after the addition of pseudin-2 or melittin. At a concentration of 4 μM (the MIC in PBS), pseudin-2 induced complete dissipation of membrane potential but not melittin, though both peptides induced rapid and dose-dependent depolarization in *E. coli* ATCC 25922 (Fig. 5A and B). The entrance of SYTOX Green into the cell cytosol was examined to gain insight into the extent to which the peptides induced membrane disruption. This cationic dye will not enter the cell without disruption of the inner membrane, and its fluorescence increases upon binding to cytoplasmic nucleic acids. Although pseudin-2 (4 μM) induced greater depolarization than melittin, pseudin-2 induced less uptake of SYTOX (Fig. 5C and D). In addition, pseudin-2 showed dose-dependent increases in fluorescence at concentrations up to 32 μM, while melittin induced maximum uptake of SYTOX at 4 μM. These findings suggest that the antimicrobial activity of pseudin-2 is influenced by its interaction with the bacterial membrane, and that its effects on bacterial cells differ from those of melittin.

3.6. Interaction of pseudin-2 with artificial liposomes

The secondary structure of pseudin-2 in membrane environments was analyzed from its CD spectra. As shown in Fig. 6A, pseudin-2 shows little helicity in aqueous solution, but exhibited a high degree of helicity in a membrane environment containing 50% TFE, PE/PG vesicles or PC/PE/PI/ergosterol vesicles.

To determine the accessibility of the peptides interacting with the membrane, proteolytic cleavage of NBD-labeled peptides was evaluated in the presence of artificial vesicles. The rationale for this experiment is that NBD-labeled peptides that just bind to the membrane surface will be cleaved by proteinase K, reducing the NBD-fluorescence. On the other hand, peptides that insert into the membrane will be inaccessible to proteinase K, so that their fluorescence is sustained. Fig. 6B shows the time-dependent changes in NBD-fluorescence following addition of the tested peptides to lipid vesicles. In the presence of PE/PG vesicles (7:3, w/w), NBD-melittin fluorescence declined following addition of proteinase K, while NBD-pseudin-2 and NBD-magainin 2 fluorescence was unaffected, suggesting the NBD-labeled regions of pseudin-2 and magainin 2 were hidden within the lipid bilayer. In addition, the fluorescence of all three NBD-peptides was protected in the presence of PC/PE/PI/ergosterol (5:4:1:2, w/w/w/w) vesicles, a model of fungal membrane (data not shown). We suggest that, like to magainin 2, pseudin-2 is able to insert into both bacterial and fungal membranes.

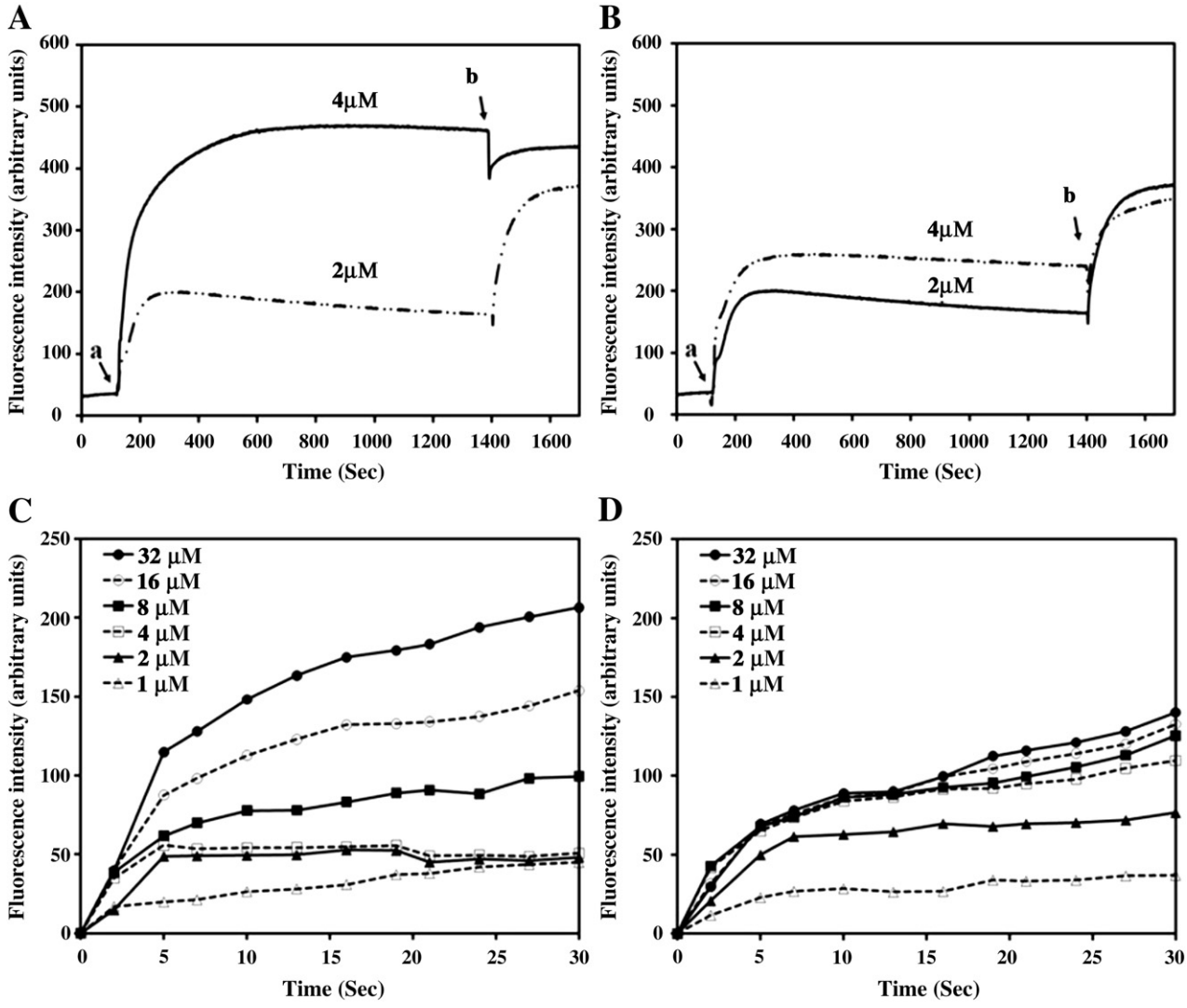

Fig. 5. Time-dependent depolarization of *E. coli* cells and influx of SYTOX Green. (A and B) Bacteria in mid-logarithmic phase were adjusted to $OD_{600} = 0.05$ and pre-equilibrated for 60 min with $diSC_3 5$. Pseudin-2 (A) or melittin (B) was then added (arrow a) to the indicated concentrations while continuously monitoring fluorescence (Ex. 622 nm and Em. 670 nm). Triton X-100 was then added (arrow b) to obtain maximum depolarization. (C and D) *E. coli* (2×10^7 cells/ml) were incubated with 1 μM SYTOX Green for 15 min. Psuedin-2 (C) or melittin (D) was added when basal fluorescence was reached a steady state, after which fluorescence was measured at the indicated times (Ex. 485 nm and Em. 520 nm).

To further examine the action of pseudin-2 in these membranes, the abilities pseudin-2, magainin 2 and melittin to induce leakage of calcein trapped within artificial lipid vesicles were compared (Fig. 6C and D). At a peptide/lipid molar ratio of 0.05, pseudin-2, magainin 2 and melittin caused the release of ~90%, 87% and 68% of the trapped calcein, respectively, from PE/PG vesicles. On the other hand, maximum leakages from PC/PE/PI/ergosterol vesicles were observed at a peptide/lipid molar ratio of 0.2, which suggests pseudin-2 was more active against bacterial cells than fungal cells.

3.7. Pseudin-2-induced pore formation

To directly observe the mode of action of pseudin-2 in artificial lipid vesicles under microscopy, GUVs were prepared either using rhodamine-labeled lipid or with entrapped CF. Photomicrographs of the GUVs showed a high degree of phase contrast due to the difference in density between the sucrose solution inside the vesicles and the glucose solution outside (Fig. 7A-(1)). After addition of pseudin-2, a time-dependent reduction in fluorescence intensity occurred over a period of 10 min in GUV composed of PE/PG/Rho-PE lipids (Fig. 7A). Because the illumination needed for fluorescence microscopy can cause a gradual reduction in fluorescence intensity due to photobleaching of rhodamine, as a control we monitored the changes in fluorescence intensity under the same conditions in the absence of paseudin-2 (Fig. 7B). Although photobleaching caused a slight decline in rhodamine fluorescence, comparison of Fig. 7A and B shows that there was a markedly greater reduction in fluorescence in the presence of pseudin-2. Moreover, exposing CF-containing GUVs to pseudin-2 also elicited a rapid reduction in fluorescence intensity (Fig. 7C). The CF fluorescence was completely lost within 7 min, though the photomicrograph in Fig. 7C-(2) shows that the GUV remained intact after 10 min in the presence of pseudin-2, but with low phase contrast. This suggests pseudin-2 formed pores allowing equilibration of the solutions inside and outside the vesicles. Pseudin-2 had similar effects on GUVs composed of PC/PE/PI/ergosterol (data not shown), suggesting pseudin-2 forms pores in both bacterial and fungal membranes.

3.8. The size of pores formed by pseudin-2 in live cells and artificial liposomes

To estimate the size of the pores formed by pseudin-2 in live cells, we visualized the influx of soluble fluorescent markers of various sizes under CLSM. We found that upon addition of pseudin-2 to *C. albicans*

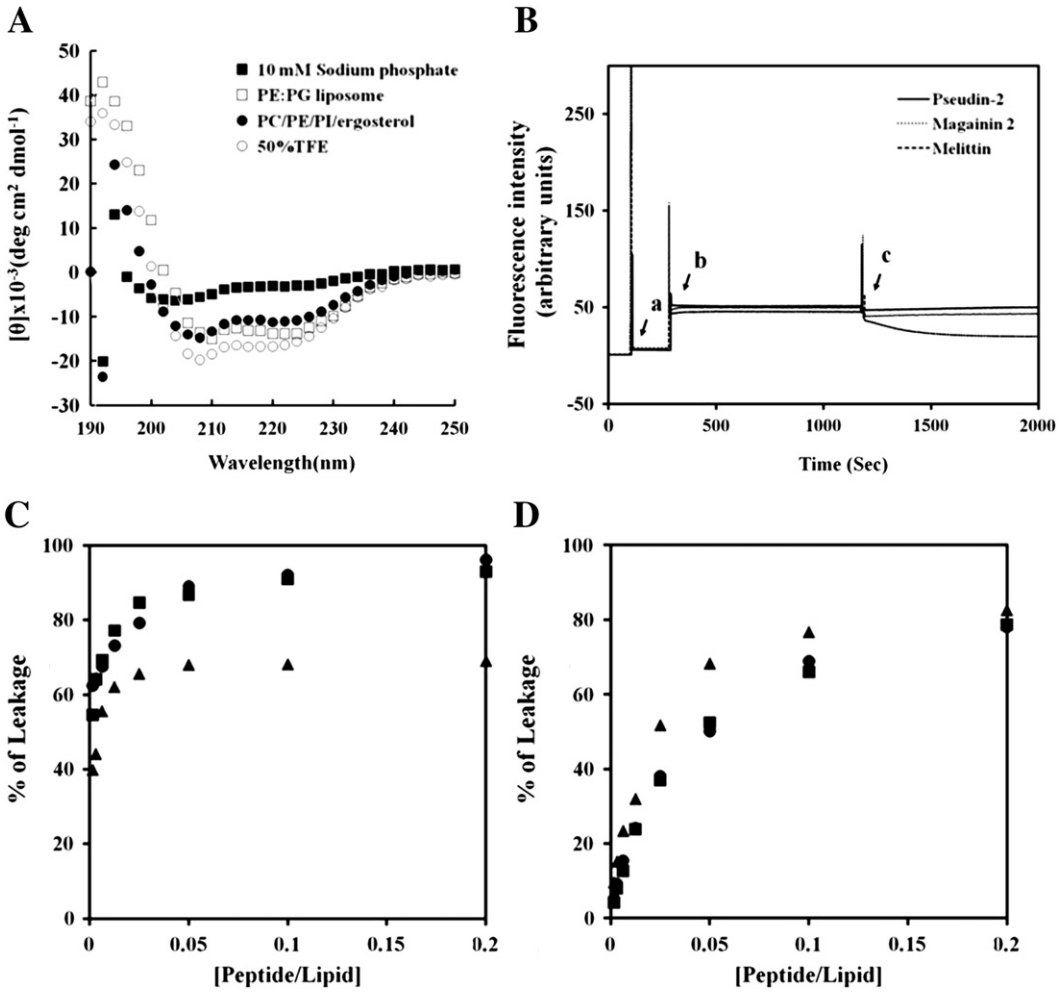

Fig. 6. Secondary structure, accessibility, and permeation of pseudin-2 in membrane environments. (A) CD spectra of pseudin-2 (30 μM) in 50% TFE and liposomes. (B) Protection of NBD-labeled pseudin-2, magainin 2 and melittin against proteolytic digestion in the presence of PE/PG liposomes: a, b, and c indicate the addition of NBD-peptide (0.1 μM), PE/PG liposomes (50 μM) and proteinase K, respectively. Fluorescence was monitored at 530 nm with excitation at 470 nm. (C and D) Peptide-induced calcein release. Peptides were added to calcein-containing PE/PG (C) and PC/PE/PI/ergosterol (D) LUVs (final concentration, 2.5 μM): ■, pseudin-2; ●, magainin 2; ▲, melittin.

(Fig. 8A) or *E. coli* (Fig. 8B) cells, calcein (~1 nm) or FD4 (diameter, ~2.8 nm) permeated into the cytoplasm. By contrast, FD10 (diameter, ~4.6 nm) did not enter the cytoplasm, though of the interaction of pseudin-2 with the cell membranes was confirmed using Rho-pseudin-2. This suggests that the pores are smaller than 4.6 nm. We also estimated pore size in artificial vesicles by assessing pseudin-2-induced release of the aforementioned markers. Calcein- and FD-containing PE/PG liposomes were incubated with 1.25 or 5 μM peptide (peptide/lipid ratio = 0.05 and 0.2), while PC/PE/PI/ergosterol liposomes were incubated with 5 and 10 μM peptide (peptide/lipid ratio = 0.2 and 0.4). Pseudin-2 caused a clear release of calcein and FD4, but not FD10, which was consistent with the findings in live cells (Fig. 8C and D). Similarly, melittin and magainin 2 also created pores that were smaller than 4.6 nm.

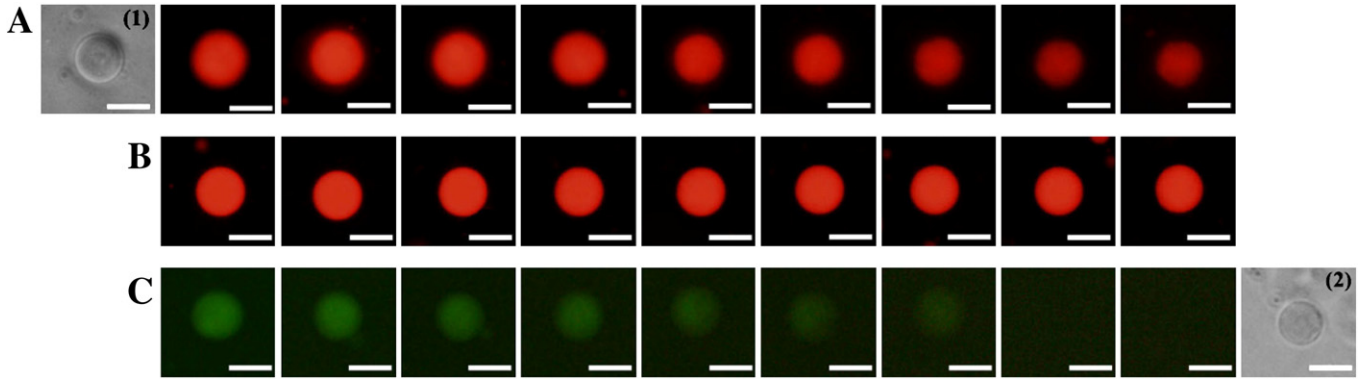

Fig. 7. (A) Time-dependent leakage of CF from Rho-PE/PE/PG GUVs in the presence of pseudin-2. (B) Photobleaching of rhodamine fluorescence in the absence of pseudin-2. (C) Time-dependent leakage of calcein from PE/PG GUVs in the presence of pesudin-2. Scale bar, 25 μm.

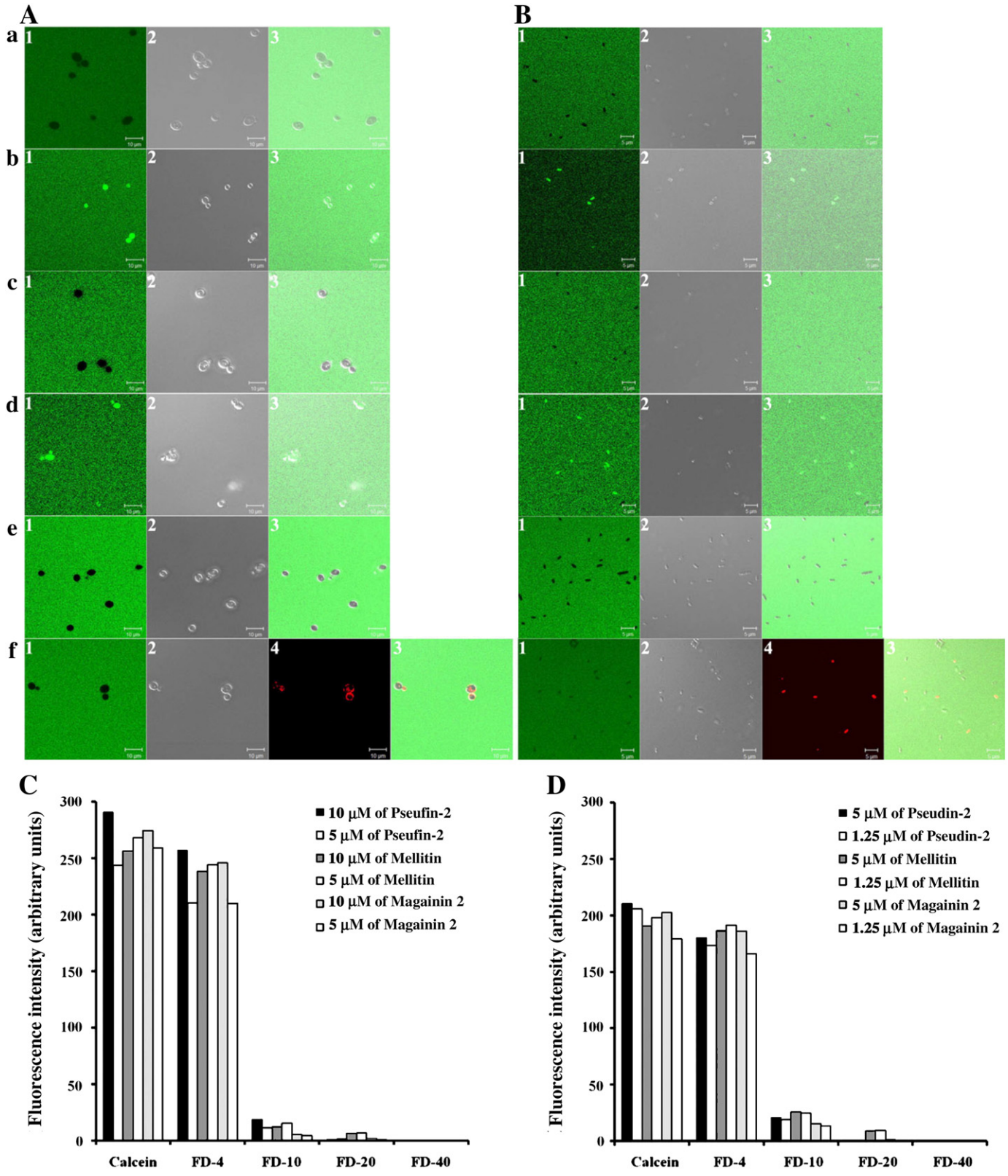

Fig. 8. Permeabilization of membranes by pseudin-2 in live cells (A and B) or liposomes (C and D). *Candida albicans* (A) or *E. coli* (B) cells were incubated with calcein (a and b), FD4 (c and d) or FD10 (e and f) in the absence (a, c and e) and presence (b, d and f) of the indicated peptide at its MIC. From left to light: 1, Calcein/FITC; 2, differential interference contrast; 3, merged image; 4, TAMRA. (C and D) Percent leakage of fluorescent marker from PE/PG (C) and PC/PE/PI/ergosterol (D) liposomes after addition of pseudin-2.

3.9. Binding of pseudin-2 to intracellular RNA

Given the concentration-dependent translocation of pseudin-2 into the cytoplasm of bacterial and fungal cells shown in Fig. 3, we also examined the binding to intracellular DNA and RNA. Pseudin-2 was mixed with a fixed amount of plasmid DNA (pDNA, 200 ng) or RNA (10 μg), after which the complexes were electrophoresed on agarose gels. A shift in the RNA band was detected at a peptide/RNA weight

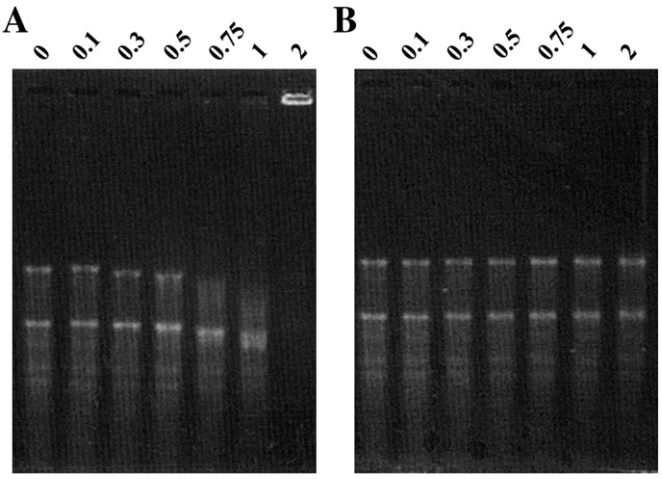

Fig. 9. Gel retardation assay showing the binding of pseudin-2 to RNA. The peptide/RNA ratios are shown at the top.

ratio of 0.3, and complete retardation of the RNA was seen at a weight ratio of 2, indicating aggregation of the RNA with pseudin-2 (Fig. 9A). On the other hand, no band shift was seen when RNA was mixed with magainin 2 (Fig. 9B), indicating RNA and magainin 2 do not interact. Pseudin-2 had no effect on the migration of pDNA, even at a peptide/pDNA weight ratio of 4 (data not shown), which suggests pseudin-2 does not bind to DNA.

4. Discussion

Previous studies reported that pseudin-2 has greater potency against Gram-negative than Gram-positive bacteria [8] and that it stimulates the release of insulin from clonal BRIN-BD11 insulinoma-derived cells [9]. These findings were subsequently confirmed [31], but the mode of action has remained unclear. In the present study, therefore, we focused on the mode of antimicrobial action of pseudin-2 in live cells and artificial membranes. Moreover, because the features and modes of action of two other AMPs, melittin and magainin 2, are relatively well-characterized, we employed them as controls against which pseudin-2 was compared.

In antimicrobial assay of AMPs, the salinity of the buffer was important, because it is one of considered factors when AMP is developed to a pharmaceutical drug containing topical, oral, systemic use. Our results of *in vitro* antimicrobial assay in both low and high ionic strength buffer with 10% culture media revealed that antimicrobial activity of pseudin-2 was almost maintained although that was slightly reduced against some bacteria. This likely reflects the fact that high salinity had no effect on the secondary structure of pseudin-2 in aqueous solution (Fig. 2B). Although the lytic activity of pseudin-2 is reportedly less effective against Gram-positive than Gram-negative bacteria [8,31], we found that it was effective against most Gram-positive bacteria, with the exception of *S. aureus* (Table 1). We suggest that psuedin-2 may induce boundary defects in the anionic lipid membranes of *S. aureus* and *S. epidermidis*, since *Staphylococcus* species contain little or no zwitterionic PE [32]. In fact, the lytic activity of pseudin-2 against *S. aureus* was low, as compared to its potent activity against *B. subtilis*, which has a high PE content. This is consistent with the earlier finding that the membrane PE content is a major determinant of the antibacterial activity of certain antimicrobial agents and peptides [33,34]. PE has an intrinsic negative curvature giving it a strong tendency to form inverted phases, which promotes formation of nonlamellar structures [33], and its headgroups are smaller than those of other phospholipids. Given the saline-independence of its antimicrobial activity, we suggest that the action of pseudin-2 on the cytoplasmic membrane is independent upon its charge (i.e., electrostatic force between a cationic peptide and the anionic membrane) but rather on its hydrophobicity (i.e., hydrophobic interaction between hydrophobic amino acids and the fatty acids of the lipid tails), which significantly impacts its initial interaction with the cell membrane and subsequent pore formation and translocation.

The bactericidal activity of pseudin-2 was confirmed in assays of its killing kinetics with two strains of *E. coli*, which showed that cell viability was significantly reduced within 40 min. In addition, pseudin-2 and melittin have the same MIC with *E. coli*, but the killing kinetics of pseidin-2 were slower than those of melittin, which suggests that a different effect of pseudin-2 contributes its killing action. This notion is supported by that Rho-pseudin-2 localized mainly in the membrane or cytoplasm of both *E. coli* and *C. albicans*, depending upon its concentration. This suggests that pseudin-2's bactericidal activity reflects both an action at the membrane and an intracellular action at cytoplasm.

Before studying mechanism of pseudin-2, we first investigated its structure and organization in aqueous solution. Melittin monomers aggregate into tetramers in aqueous solution, depending upon the ionic strength and peptide concentration [35,36], and this self-assembly is believed to be important for its membranolytic activity [37]. Pseudin-2 induced to alpha-helical structure, concentration-dependently. We suggest that pseudin-2 peptides are aggregated or self-associated by their hydrophobic amino acids, because each peptides are closed in high concentration. Its potent antimicrobial activity in high salinity was consistent that its structure did not change by increasing NaCl up to a concentration of 100 mM. Aggregation of pseudin-2 was confirmed by the significant change in fluorescence intensity induced by proteolytic enzymes, like a previous report [38]. Rho-pseudin-2 fluorescence significantly differed before or after enzymatic degradation by proteinase K, whereas there was little change in the fluorescence of melittin, which is not easily cleaved by proteinase K (Fig. 2C). This implies that melittin exists as an ordered self-aggregate in which the melittin monomers are tightly linked, while pseudin-2 is randomly aggregated in aqueous solution.

Consequently, an initial step for antimicrobial agents is generally passage through the cell wall, which act as protective barriers against antibiotics and/or as effector molecules activating the innate immune system during bacterial infection [39–41]. LPS contains diphosphoryl head groups and acyl chains, which possess a net anionic charge and hydrophobic characteristics, respectively. Many host-defense peptides initially bind to LPS through electrostatic interactions with its anionic head groups, then form a stable complex through hydrophobic interactions with its fatty acyl chains, ultimately disrupting the LPS layer [42]. But, pseudin-2 did not interact with head groups of LPS (Supplementary Fig. 1). Interestingly, however, its fluorescence intensity was increased when LPS was added to Rho-pseudin-2, suggesting that the aggregated pseudin-2 peptides dissociate into monomers upon interaction with LPS (Fig. 4A). It has been proposed that the bulky compounds between LPS and peptides are unable to pass through the cytoplasmic membrane [43]. In a similar vein, our present findings suggest the randomly aggregated pseudin-2 dissociate upon interaction with the fatty acyl chains of LPS, enabling the monomers to insert into the interior of the bilayer, even though they do not effectively neutralize the LPS.

Antimicrobial action of some AMPs involves to insertion into the cytoplasmic membrane with pore formation and resultant dissipation of the membrane potential and disruption of lipid asymmetry [44–48]. We examined the interaction of pseudin-2 with the membrane using both bacterial cells and artificial vesicles. We found that pseudin-2 completely dissipated the membrane potential of *E. coli* at its MIC, whereas melittin induced minimal depolarization (5A and B). Pseudin-2 also induced increasing efflux of SYTOX green (Fig. 5C and D), concentration-dependently, indicating that its effectiveness in membrane occurred in both the outer and inner membrane. In

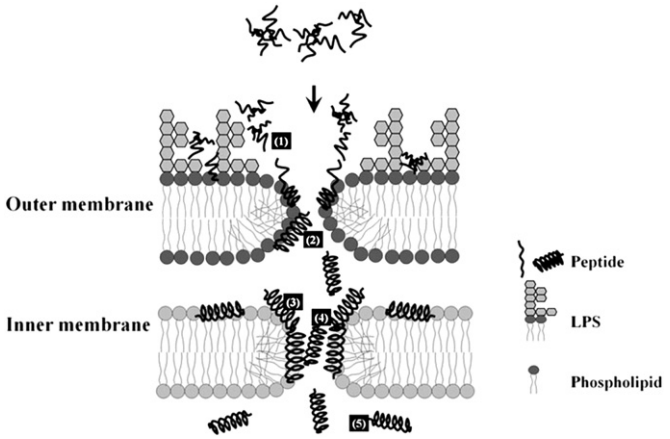

Fig. 10. Mode of action of pseudin-2 in bacterial cell membranes. (1) Dissociation of randomly aggregated pseudin-2 upon interaction with the acyl chains of LPS, (2) induction of an α-helical structure and pore formation by interaction with the inner leaflet lipids of LPS, (3) binding to the outer leaflet lipids of the inner membrane, (4) formation of a toroidal pore, (5) permeation of the pore by other pseudin-2 molecules.

previous reports, melittin did not elicit complete leakage from PG vesicles, and leakage was accompanied by membrane aggregation [49,50].

Pseudin-2 adopts a helical structure in membrane-mimetic environments, such as TFE/water (50%, v/v), PE/PG (7:3, w/w) and PC/PE/PI/ergosterol (5:4:2:1, w/w/w/w) (Fig. 6A). NBD-pseudin-2 clearly resisted cleavage by proteinase K when it was bound to negatively charged vesicles (PE/PG) (Fig. 6B), suggesting that the N-terminus of pseudin-2 inserts into the lipid bilayer. This is similar to the action of magainin 2, which forms pores in negatively charged membranes [44], but differs from the parallel binding of melittin, which prevents both the insertion of other peptide molecules and pore formation [51]. Pseudin-2 induced faster and more extensive calcein release from PE/PG vesicles than PC/PE/PI/ergosterol vesicles (Fig. 6C and D) at low peptide/lipid molar ratios is consistent with the stronger effect of pseudin-2 against bacterial cells than fungal cells.

Attenuation change of artificial vesicles with peptides was proposed that pseudin-2 act by pore formation in both PE/PG and PC/PE/PI/ergosterol vesicles (Supplementary Fig. 2). In addition, "pore formation" mechanism of pseudin-2 was confirmed by GUV experiments and the diameters of pores formed in *E. coli* and *C. albicans* ranged between 2.8 and 4.8 nm, which is similar to the pores formed in PE/PG and PC/PE/PI/ergosterol vesicles, as well as to the pores formed by magainin 2 [27]. Magainin 2 does not bind to DNA or RNA [44] although it enters into cytoplasm. Interestingly, in this study, we found that pseudin-2 peptides entering the cytoplasm through pores formed by themselves specifically bound to RNA, which would be expected to inhibit protein synthesis. This action is able to describe its later killing kinetic and the increased efflux of SYTOX green in over MIC value.

In conclusion, the mode of action of pseudin-2 can be describe by a five-step process (Fig. 10): (1) dissociation of randomly aggregated peptides upon binding to the lipid core of LPS; (2) formation of an α-helical structure through interaction with inner-leaflet lipids of the outer membrane, and subsequent pore formation; (3) transfer of peptides through the pores formed and binding to outer-leaflet lipids of the inner membrane; (4) formation of pores in the inner membrane; and (5) entrance of pseudin-2 into the cytoplasm, where it binds with RNA. Characterization of native AMPs will necessarily precede the development of therapeutic agents. The results of the present study shed new light on the action of pseudin-2 and could aid in the design of new agents by furthering the development of pseudin-2 analogues with enhanced antimicrobial activity and reduced cytotoxicity.

Acknowledgements

This work was supported by a Korean Research Foundation Grant funded by the Korean Government [KRF-2008-359-C00022].

Appendix A. Supplementary data

Supplementary data to this article can be found online at doi:10.1016/j.bbamem.2010.08.023.

References

[1] M. Zasloff, Antimicrobial peptides of multicellular organisms, Nature 415 (2002) 389–395.
[2] M.R. Yeaman, N.Y. Yount, Mechanisms of antimicrobial peptide action and resistance, Pharmacol. Rev. 55 (2003) 27–55.
[3] K.A. Brogden, Antimicrobial peptides: pore formers or metabolic inhibitors in bacteria? Nat. Rev. Microbiol. 3 (2005) 238–250.
[4] Y. Shai, Mechanism of the binding, insertion and destabilization of phospholipid bilayer membranes by alpha-helical antimicrobial and cell non-selective membrane-lytic peptides, Biochim. Biophys. Acta 1462 (1999) 55–70.
[5] M.P. Boland, F. Separovic, Membrane interactions of antimicrobial peptides from Australian tree frogs, Biochim. Biophys. Acta 1758 (2006) 1178–1183.
[6] J.D. Hale, R.E. Hancock, Alternative mechanisms of action of cationic antimicrobial peptides on bacteria, Expert Rev. Anti Infect. Ther. 5 (2007) 951–959.
[7] A.C. Rinaldi, Antimicrobial peptides from amphibian skin: an expanding scenario, Curr. Opin. Chem. Biol. 6 (2002) 799–804.
[8] L. Olson, A. Soto, F.C. Knoop, J.M. Conlon, Pseudin-2: an antimicrobial peptide with low hemolytic activity from the skin of the paradoxical frog, Biochem. Biophys. Res. Commun. 288 (2001) 1001–1005.
[9] Y.H. Abdel-Wahab, G.J. Power, M.T. Ng, P.R. Flatt, J.M. Conlon, Insulin-releasing properties of the frog skin peptide pseudin-2 and its [Lys18]-substituted analogue, Biol. Chem. 389 (2008) 143–148.
[10] J.K. Ghosh, D. Shaool, P. Guillaud, L. Ciceron, D. Mazier, I. Kustanovich, Y. Shai, A. Mor, Selective sytotoxicity of dermaseptin S3 toward intraerythrocytic *Plasmodium falciparum* and the underlying molecular basis, J. Biol. Chem. 272 (1997) 31609–31616.
[11] D. Rapaport, Y. Shai, Aggregation and organization of pardaxin in phospholipid membranes, J. Biol. Chem. 267 (1992) 6502–6509.
[12] S.C. Park, M.H. Kim, M.A. Hossain, S.Y. Shin, Y. Kim, L. Stella, J.D. Wade, Y. Park, K.S. Hahm, Amphipathic alpha-helical peptide, HP (2-20), and its analogues derived from *Helicobacter pylori*: pore formation mechanism in various lipid compositions, Biochim. Biophys. Acta 1778 (2008) 229–241.
[13] S.C. Park, J.R. Lee, S.O. Shin, Y. Park, S.Y. Lee, K.S. Hahm, Characterization of a heat-stable protein with antimicrobial activity from *Arabidopsis thaliana*, Biochem. Biophys. Res. Commun. 362 (2007) 562–567.
[14] Y.H. Chen, J.T. Yang, K.H. Chau, Determination of the helix and beta form of proteins in aqueous solution by circular dichroism, Biochemistry 13 (1974) 3350–3359.
[15] H. Meng, K. Kumar, Antimicrobial activity and protease stability of peptides containing fluorinated amino acids, J. Am. Chem. Soc. 129 (2007) 15615–15622.
[16] Z. Oren, J.C. Lerman, G.H. Gudmundsson, B. Agerberth, Y. Shai, Structure and organization of the human antimicrobial peptide LL-37 in phospholipid membranes: relevance to the molecular basis for its non-cell-selective activity, Biochem. J. 341 (1999) 501–513.
[17] N. Papo, Z. Oren, U. Pag, H.G. Sahl, Y. Shai, The consequence of sequence alteration of an amphipathic α-helical antimicrobial peptide and its diastereomers, J. Biol. Chem. 277 (2002) 33913–33921.
[18] M.L. Mangoni, N. Papo, D. Barra, M. Simmaco, A. Bozzi, A. Di Giulio, A.C. Rinaldi, Effects of the antimicrobial peptide temporin L on cell morphology, membrane permeability and viability of *Escherichia coli*, Biochem. J. 380 (2004) (2004) 859–865.
[19] K. Marynka, S. Rotem, I. Portnaya, U. Cogan, A. Mor, In vitro discriminative antipseudomonal properties resulting from acyl substitution of N-terminal sequence of dermaseptin S4 derivatives, Chem. Biol. 14 (2007) 75–85.
[20] W.S. Jang, S.C. Lee, Y.S. Lee, Y.P. Shin, K.H. Shin, B.H. Sung, B.S. Kim, S.H. Lee, I.H. Lee, Antimicrobial effect of halocidin-derived peptide in a mouse model of *Listeria* infection, Antimicrob. Agents Chemother. 51 (2007) 4148–4156.
[21] Y. Rosenfeld, D. Barra, M. Simmaco, Y. Shai, M.L. Mangoni, A synergism between temporins toward Gram-negative bacteria overcomes resistance imposed by the lipopolysaccharide protective layer, J. Biol. Chem. 281 (2006) 28565–28574.
[22] S.C. Park, J.R. Lee, S.O. Shin, J.H. Jung, Y.M. Lee, H. Son, Y. Park, S.Y. Lee, K.S. Hahm, Purification and characterization of an antifungal protein, C-FKBP, from Chinese cabbage, J. Agric. Food Chem. 55 (2007) 5277–5281.
[23] N. Asthana, S.P. Yadav, J.K. Ghosh, Dissection of antibacterial and toxic activity of melittin, J. Biol. Chem. 279 (2004) 55042–55050.
[24] J.K. Ghosh, S.G. Peisajovich, M. Ovadia, Y. Shai, Serum-induced leakage of liposome contents, J. Biol. Chem. 273 (1998) 27182–27190.
[25] M.I. Angelova, D.S. Dimitrov, Liposome electroformation, Faraday Discuss. Chem. Soc. 81 (1986) 127–131.
[26] D.J. Estes, M. Mayer, Electroformation of giant liposomes from spin-coated films of lipids, Colloids Surf. B Biointerfaces 42 (2005) 115–123.

[27] Y. Imura, N. Choda, K. Matsuzaki, Magainin 2 in action: distinct modes of membrane permeabilization in living bacterial and mammalian cells, Biophys. J. 95 (2008) 5757–5765.
[28] O.S. Belokoneva, H. Satake, E.L. Mal'tseva, N.P. Pal'mina, E. Villegas, T. Nakajima, G. Corzo, Pore formation of phospholipid membranes by the action of two hemolytic arachnid peptides of different size, Biochim. Biophys. Acta 1664 (2004) 182–188.
[29] J.C.M. Stewart, Colorimetric determination of phospholipids with ammonium ferrothiocyanate, Anal. Biochem. 104 (1080) 10-14.
[30] C.H. Hsu, C. Chen, M.L. Jou, A.Y.L. Lee, Y.C. Lin, Y.P. Yu, W.T. Huang, S.H. Wu, Structural and DNA-binding studies on the bovine antimicrobial peptide, indolicidin: evidence for multiple conformations involved in binding to membranes and DNA, Nucleic Acids Res. 33 (2005) 4053–4064.
[31] T. Pál, A. Sonnevend, S. Galadari, J.M. Conlon, Design of potent, non-toxic antimicrobial agents based upon the structure of the frog skin peptide, pseudin-2, Regul. Pept. 129 (2005) 85–91.
[32] R.M. Epand, S. Rotem, A. Mor, B. Berno, R.F. Epand, Bacterial membranes as predictors of antimicrobial potency, J. Am. Chem. Soc. 130 (2008) 14346–14352.
[33] L. Yang, V.D. Gordon, A. Mishra, A. Som, K.R. Purdy, M.A. Davis, G.N. Tew, G.C. Wong, Synthetic antimicrobial oligomers induce a composition-dependent topological transition in membranes, J. Am. Chem. Soc. 129 (2007) 12141–12147.
[34] R.F. Epand, M.A. Schmitt, S.H. Gellman, R.M. Epand, Role of membrane lipids in the mechanism of bacterial species selective toxicity by two alpha/beta-antimicrobial peptides, Biochim. Biophys. Acta 1758 (2006) 1343–1350.
[35] M.D. Kemple, P. Buckley, P. Yuan, F.G. Prendergast, Main chain and side chain dynamics of peptides in liquid solution from 13C NMR: melittin as a model peptide, Biochemistry 36 (1997) 1678–1688.
[36] M. Iwadate, T. Asakura, M.P. Williamson, The structure of the melittin tetramer at different temperatures: an NOE-based calculation with chemical shift refinement, Eur. J. Biochem. 257 (1998) 479–487.
[37] S. Frey, L.K. Tamm, Orientation of melittin in phospholipid bilayers. A polarized attenuated total reflection infrared study, Biophys. J. 60 (1991) 922–930.
[38] J.K. Ghosh, D. Shaool, P. Guillaud, L. Ciceron, D. Mazier, I. Kustanovich, Y. Shai, A. Mor, Selective cytotoxicity of dermaseptin S3 toward intraerythrocytic *Plasmodium falciparum* and the underlying molecular basis, J. Biol. Chem. 272 (1997) 31609–31616.
[39] A. Giacometti, O. Cirioni, R. Ghiselli, F. Mocchegiani, M.S. Del Prete, C. Viticchi, W. Kamysz, E. Lempicka, V. Saba, G. Scalise, Potential therapeutic role of cationic peptides in three experimental models of septic shock, Antimicrob. Agents Chemother. 46 (2002) 2132–2136.
[40] M. Gough, R.E. Hancock, N.M. Kelly, Antiendotoxin activity of cationic peptide antimicrobial agents, Infect. Immun. 64 (1996) 4922–4927.
[41] R.E. Hancock, M.G. Scott, The role of antimicrobial peptides in animal defenses, Proc. Natl. Acad. Sci. USA 97 (2000) 8856–8861.
[42] P. Li, T. Wohland, B. Ho, J.L. Ding, Perturbation of lipopolysaccharide (LPS) micelles by Sushi 3 (S3) antimicrobial peptide, J. Biol. Chem. 279 (2004) 50150–50156.
[43] N. Papo, Y. Shai, A molecular mechanism for lipopolysaccharide protection of Gram-negative bacteria from antimicrobial peptides, J. Biol. Chem. 280 (2005) 10378–10387.
[44] K. Matsuzaki, Magainin as paradigm for the mode of action of pore forming polypeptides, Biochim. Biophys. Acta 1376 (1998) 391–400.
[45] T.J. Falla, D.N. Karunaratne, R.E. Hancock, Mode of action of the antimicrobial peptide indolicidin, J. Biol. Chem. 271 (1996) 19298–19303.
[46] D. Gidalevitz, Y. Ishitsuka, A.S. Muresan, O. Konovalov, A.J. Waring, R.I. Lehrer, K.Y. C. Lee, Interaction of antimicrobial peptide protegrin with biomembranes, Proc. Natl. Acad. Sci. USA 100 (2003) 6302–6307.
[47] L. Yang, V.D. Gordon, D.R. Trinkle, N.W. Schmidt, M.A. Davis, C. DeVries, A. Som, J.E. Cronan Jr., G.N. Tew, G.C. Wong, Mechanism of a prototypical synthetic membrane-active antimicrobial: efficient hole-punching via interaction with negative intrinsic curvature lipids, Proc. Natl. Acad. Sci. USA 105 (2008) 20595–20600.
[48] A. Makovitzki, D. Avrahami, Y. Shai, Ultrashort antibacterial and antifungal lipopeptides, Proc. Natl. Acad. Sci. USA 103 (2006) 15997–16002.
[49] S.C. Park, J.Y. Kim, S.O. Shin, C.Y. Jeong, M.H. Kim, S.Y. Shin, G.W. Cheong, Y. Park, K.S. Hahm, Investigation of toroidal pore and oligomerization by melittin using transmission electron microscopy, Biochem. Biophys. Res. Commun. 343 (2006) 222–228.
[50] G. van den Bogaart, J.T. Mika, V. Krasnikov, B. Poolman, The lipid dependence of melittin action investigated by dual-color fluorescence burst analysis, Biophys. J. 93 (2007) 154–163.
[51] G. van den Bogaart, J.V. Guzmán, J.T. Mika, B. Poolman, On the mechanism of pore formation by melittin, J. Biol. Chem. 283 (2008) 33854–33857.